DOI: 10.1002/chem.200902684

Analysis of a Pentacoordinate Iron Dicarbonyl as Synthetic Analogue of the Hmd or Mono-Iron Hydrogenase Active Site**

Tianbiao Liu,[a] Bin Li,[c] Codrina V. Popescu,*[b] Andrey Bilko,[b] Lisa M. Pérez,[a] Michael B. Hall,*[a] and Marcetta Y. Darensbourg*[a]

Abstract: Pentacoordinate iron dicarbonyls, $(NS)Fe(CO)_2P$ (NS = 2-amidothiophenylate, $P = PCy_3$ (**4**), PPh_3, (**5**), and $P(OEt)_3$ (**6**)) were prepared as potential biomimetics of the active site of the mono-iron hydrogenase, [Fe]-H_2ase. Full characterization including X-ray diffraction, density functional theory (DFT) computations, and Mössbauer studies for complexes **5** and **6** find that, despite similar infrared ν(CO) pattern and absorption frequencies as the active site of the [Fe]-H_2ase, the geometrical distortions towards trigonal bipyramidal, the negative isomer shift parameters, and the differences in CO-uptake reactivity are due to the "non-innocence" of the NS ligand. Ligand-based protonation with a strong acid, $HBF_4{\cdot}Et_2O$, interrupted the extensive π-delocalization over Fe and NS ligand of complex **4** and switched on CO uptake (1 bar) to form a CO adduct, *mer*-$[(H\text{-}NS)Fe(CO)_3(PCy_3)]^+$ or **4**(CO)-H^+. The extrinsic CO is reversibly removed on deprotonation with Et_3N to regenerate complex **4**. In a ^{13}CO atmosphere, concomitant CO uptake by **4**-H^+ and exchange with intrinsic CO groups provide a facile route to ^{13}C-labeled **4**(CO)-H^+ and, upon deprotonation, ^{13}C-labeled complex **4**. DFT calculations show substantial Fe character in the LUMO of **4**-H^+ typical of the d^6 Fe^{II} in a regular square-pyramidal geometry. Thus, the Lewis acidity of **4**-H^+ makes it amenable for CO binding, whereas the dianionic NS ligand renders the iron center of **4** insufficiently electrophilic and largely of Fe^I character.

Keywords: hydrogenases · iron · non-innocent-ligand CO exchange · synthetic analogues

Introduction

The hydrogenase active sites and the chemistry they perform have inspired synthetic chemists in attempts to produce small molecule analogues[1–3] as potential base–metal catalysts for H_2 uptake, H_2 production, or, in the case of the mono-iron hydrogenase, [Fe]-H_2ase, H_2 activation for a hydride reduction process.[4–9] Recent studies including X-ray diffraction,[7,9] spectroscopies,[4,5] and DFT modeling[10] suggest the active site of the [Fe]-H_2ase consists of a low-spin Fe^{II}, two *cis*-oriented CO ligands, a cysteinyl-S, an organic pyridone bidentate ligand (N and acyl carbon), and a H_2O (or an open site) *trans* to the acyl group as sketched in Figure 1.

Different from the [FeFe]- and [NiFe]-H_2ases that directly utilize H_2 and H^+ as substrates in hydrogen metabolism ($H_2 = 2H^+ + 2e^-$), the [Fe]-H_2ase (alternatively called Hmd or H_2-forming methylene-H_4MPT dehydrogenase) catalyzes the reduction of N^5,N^{10}-methenyl-tetrahydromethanopterin (methenyl-H_4MPT^+, or H_4MPT^+) with H_2 to N^5,N^{10}-methylene-tetrahydromethanopterin (methylene-H_4MPT, or H_4MPT) and a proton (Figure 1).[6,8] The [Fe]-H_2ase catalyzes isotopic exchange in T_2/H_2O or D_2/H_2O mixtures and the conversion of *para*-H_2/*ortho*-H_2 only in the presence of H_4MPT^+ while the [NiFe]- and [FeFe]-H_2ases catalyze the same reactions without an exogenous electron acceptor/donor.[8] Illustrated in Figure 1 is an appealing ter-

[a] T. Liu, Dr. L. M. Pérez, Prof. M. B. Hall, Prof. M. Y. Darensbourg
Department of Chemistry, Texas A&M University
College Station, TX 77843 (USA)
Fax: (+1) 979-845-0158
E-mail: marcetta@mail.chem.tamu.edu

[b] Prof. C. V. Popescu, A. Bilko
Department of Chemistry, Ursinus College
Collegeville, PA 19426 (USA)
E-mail: cpopescu@ursinus.edu

[c] B. Li
School of Chemical Engineering and Technology, Tianjin University
Tianjin, 300072 (PR China)

[**] Hmd = H_2-forming methylene-tetrahydromethanopterin dehydrogenase.

Supporting information for this article is available on the WWW under http://dx.doi.org/10.1002/chem.200902684.

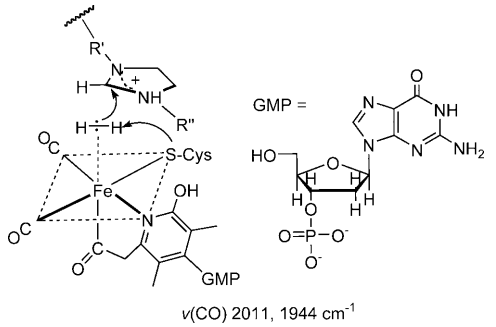

Figure 1. Formulation of the active site of the [Fe]-H_2ase and a suggested mechanism of action, that is, stereoselective hydride abstraction from (η^2 -H_2)Fe^{II} by the H_4MPT^+ substrate (see text).[8]

nary-complex mechanism put forth by Thauer, Shima, et al. that uses the d^6, Fe^{II} catalytic center as an H_2 trapping site, with the carbonium ion of the H_4MPT^+ substrate strategically positioned to abstract hydride with concurrent proton transfer to a nearby base.[6] This mechanism does not invoke an Fe–H intermediary, however, DFT calculations have suggested that a hydride transfer mechanism involving Fe–H cannot be ruled out.[10]

Synthetic analogues recently developed for the [Fe]-H_2ase include octahedral Fe^{II} dicarbonyls that mimic the denatured state of Hmd.[4,11,12] The Rauchfuss group reported a hexacoordinate $(PhS)(Ph_2PC_6H_4C(=O))Fe(CO)_3$[13] which has the acyl carbonyl built in as analogue of the CO-inhibited state.[4] A rare example of a pentacoordinate, presumably Fe^{II} dicarbonyl, is that of an (acetyl)Fe^{II} complex derived from carbonylation of a 3-coordinate Fe–Me species reported from the Holland laboratory.[14] Inspired by the report of Liaw, et al.,[15] that pentacoordinate, 16-electron Fe^{II} dicarbonyl complexes could be accessed in the presence of strong π-donor ligands such as the 2-amidothiophenolate dianion, we have developed a series of iron dicarbonyl complexes **4**, **5** and **6**. Herein, we report syntheses, electronic structures, and characterizations, including protonation-activated CO uptake and $^{12}CO/^{13}CO$ exchange, as influenced by the unique electronic makeup of the Fe(NS) unit.

Results and Discussion

Synthesis and characterization: Scheme 1 outlines a reliable procedure used to prepare $(NS)Fe(CO)_2(PR_3)$ neutral complexes; the approach is somewhat different from that of

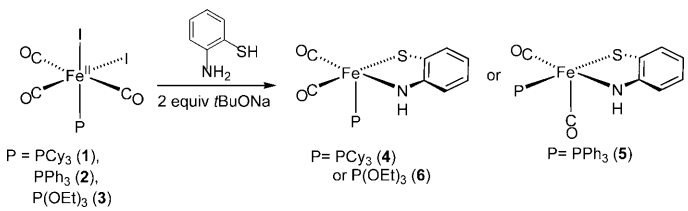

Scheme 1. One-pot synthesis of complexes **4**, **5** and **6**.

Liaw, et al. for the cyano analogue.[15] The target complexes were isolated as dark brown crystalline solids in moderate to good yields. In the case of complex **5**, the Fe^0 complex, *trans*-$[Fe(CO)_3(PPh_3)_2]$, was a substantial byproduct. Complexes **4**, **5** and **6** are air stable and may be handled for short periods at room temperature in the dark. However, their thermal and light sensitivity requires that they be stored at low (−40 °C) temperatures and always shielded from light. The light sensitivity displayed by **5** and **6** is also a characteristic of the [Fe]-H_2ase enzyme.[16] Compounds **4**, **5**, and **6** show sharp ^{31}P NMR resonances at 89.6, 97.4 and 173.6 ppm, respectively, confirming their diamagnetism. They are soluble in most organic solvents.

Figure 2 displays the ν(CO) IR spectra for which the near equal intensity of the two bands suggests *cis*-dicarbonyls are at about 90° angles. The ν(CO) band positions follow that expected for the electron-donating abilities of the phosphine ligands; those of complexes **5** and **6** (measured in CH_2Cl_2) are closest to those of the [Fe]-H_2ase active site (2011 and 1944 cm^{-1} and likewise of equal intensities).[4]

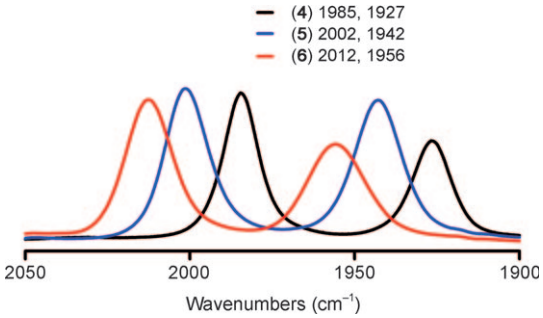

Figure 2. IR spectra (ν(CO) region) of complexes **4**, **5** and **6** in CH_2Cl_2.

Details of the X-ray diffraction studies of crystalline compounds **4** and **5** are fully described in the Supporting Information. The ORTEP drawings of the molecular structures are presented in Figure 3 so as to emphasize the square pyramidal structure of complex **5** for which analysis according to Addison's τ value[17] finds complex **5** ($\tau = 0.192$, based on α(S1-Fe-C2) = 173.9° and β(C1-Fe-Ni) = 141.0°) to be more nearly a square pyramid (similarly to Liaw's cyano complex),[15] while complex **4** ($\tau = 0.53$, based on α(S-Fe-P) = 166.5° and β(N-Fe-C1) = 155.0°) is a hybrid of square pyramidal and trigonal bipyramidal geometries.

Computational studies: These high quality crystal structures encouraged examination of the extent of light atom metric differences that might signal interruption of the aromaticity in the aryl ring and the NS ligand's "non-innocence".[18] DFT computations used in this analysis were performed with the B3LYP in a double zeta basis set for the free ligand and complexes **4**–**6**. Complex **4** was further examined with another functional and basis set (see Computational Details in the Experimental Section). The DFT-optimized structures, which agree with the corresponding crystal structures

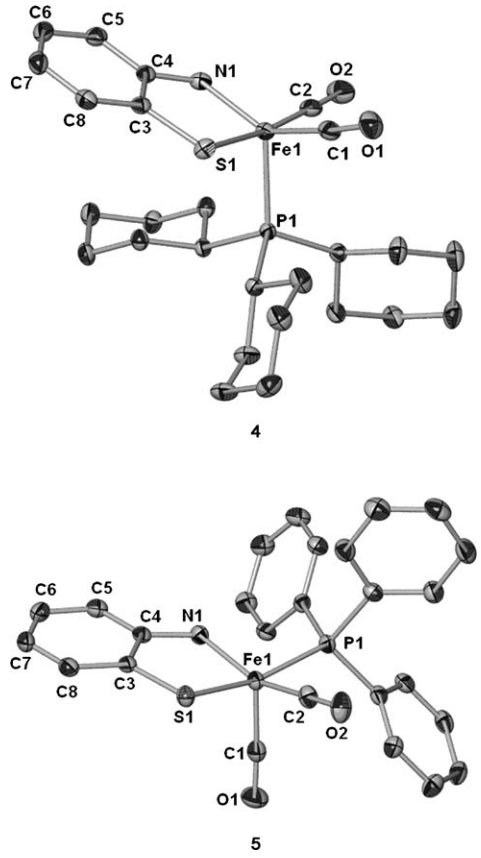

Figure 3. Molecular structures of complexes **4** (top) and **5** (bottom) as thermal ellipsoid representations, 50% probability, hydrogen atoms omitted. Selected metric parameters of **4**: Fe1–C1 1.764(2), Fe1–P1 2.248(4), Fe1–S1 2.240(4), Fe1–N1 1.855(1), C4–N1 1.374(2), C3–S1 1.724(2), C3–C4 1.409(2), C3–C8 1.411(2), C4–C5 1.420(2), C5–C6 1.380(2), C6–C7 1.401(2), C7–C8 1.381(2) Å; C1-Fe1-C2 92.20(7), S1-Fe1-N1 84.64(4), C1-Fe1-N1 140.97(6), S1-Fe1-C2 173.32(5), N1-Fe1-P1 120.21(4), S1-Fe1-P1 93.39(2), C2-Fe1-P1° 93.13(5); selected metric parameters of **5**: Fe1–C1 1.751(3), Fe1–P1 2.241(1), Fe1–S1 2.219(2), Fe1–N1 1.863(2), C4–N1 1.362(3), C3–S1 1.725(2), C3–C4 1.410(3), C3–C8 1.401(3), C4–C5 1.409(3), C5–C6 1.371(3), C6–C7 1.397(4), C7–C8 1.370(4) Å; C1-Fe1-C2 94.22(12), S1-Fe1-N1 84.63(6), C2-Fe1-N1 154.98(10), S1-Fe1-P1 166.48(3), N1-Fe1-C1 110.43(10), S1-Fe1-C 96.86(9), P1-Fe1-C1 96.62(9)°.

(see for example, Figure 4) of these complexes, were confirmed as energy minima by frequency calculations. In particular, the largest deviation of Fe–donor atom distances occur for Fe–P which is calculated to be 0.06 Å larger than the experimental value, an error that is typical for this functional and basis set. The calculated metrical details are also in good agreement for complex **5**.

In the case of complex **4**, the isomer with optimized parameters that better matched experimental data has an energy about 1–2 kcal mol^{-1} higher than the lowest energy isomer given in Figure 4. The main structural difference in the isomers lies in the N-Fe-C(1) angle of 128° in the lowest energy isomer but 138°(avg) in the isomer that better matches the experiment (141°) (see Supporting Information, Figure S1b). When the geometry was optimized for an isomer of **4** that corresponds to the geometry of **5**, a third isomer was predicted in which the PCy_3 ligand is *trans* to

	DFT	Exptl
Fe-S	2.293	2.240(4)
Fe-N	1.855	1.855(2)
Fe-P	2.307	2.248(4)
C3-S	1.753	1.724(2)
C4-N	1.392	1.374(2)
C3-C4	1.424	1.409(2)
C4-C5	1.422	1.420(2)
C5-C6	1.399	1.380(2)
C6-C7	1.420	1.401(2)
C7-C8	1.402	1.381(2)
C8-C3	1.417	1.411(2)

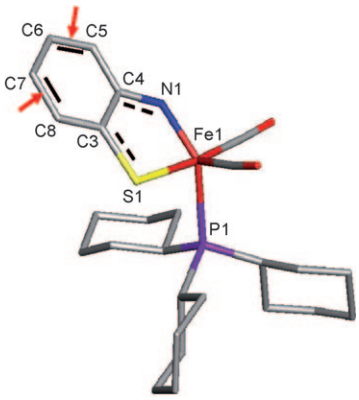

Figure 4. Comparison of DFT and experimental metric parameters for complex **4**. Additional metric parameters are in the Supporting Information.

the N rather than *trans* to the "open" site (**4**) or *trans* to the sulfur (**5**). The two calculated isomers of **4** are isoenergetic (< 0.4 kcal mol^{-1} different). Thus, alternative ligand arrangements, such as those observed for **4** and **5**, may be possible in related species.

An alternating pattern of C–C bonds in the aryl ring of the 2-amidothiophenolate ligand is found in both the calculated structures of complexes **4** and **5** and the experimental X-ray diffraction data. Furthermore, the pattern of C–C bond lengths in the "aromatic" ring shows that the C5–C6 and C7–C8 are the two shortest bonds in both the calculated and experimental structures. The other bonds are all longer; in particular C6–C7, which in a truly aromatic ring would have the same bond distances as C5–C6/C7–C8, is 0.02 Å longer than the other bonds in both the calculated and experimental structures.

In order to examine the significance of this C–C bond pattern, DFT calculations were also performed for the free NS ligand in three redox levels: the −2 amidothiophenolate (NS^{2-}), the −1 π-radical or 2-iminothionebenzosemiquinoate (NS^{-}), and the neutral 6-iminocyclohexa-2,4-dienethione forms (NS^{0}). Table 1 lists the calculated distances in the free ligand in these various possible forms and of the ligand within complexes **4** and **5**. The comparison of the bond lengths alone could lead one to conclude that the ligand within the complexes is most like the −1 π-radical. However, one should not take this to mean that the complex contains a radical ligand as an average of the dianionic amidothiolate and the neutral iminothione forms could produce a similar pattern.

According to Wieghardt et al., a bonding pattern such as that described above, that is, alternating short–long–short C–C distances in the C5–C6/C6–C7/C7–C8 positions, indicates that the 2-amidothiophenolate ligand is in a one-electron oxidized level, with substantial 2-iminothionebenzosemiquinonate, π-radical character.[18] If so, the formal charge of the Fe center of these complexes should be +1, and the observed diamagnetism would suggest that the unpaired electrons on ligand and metal are antiferromagnetically cou-

Table 1. Calculated distances [Å] within the NS ligand in three redox levels and within the ligand in complexes **4** and **5**.

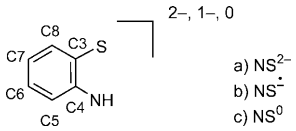

	a) NS^{2-}	b) NS^{-}	c) NS^{0}	NS in **4**	NS in **5**
C3–C4	1.493	1.482	1.512	1.424	1.425
C4–C5	1.462	1.462	1.480	1.422	1.424
C5–C6	1.414	1.388	1.364	1.399	1.398
C6–C7	1.409	1.428	1.456	1.420	1.421
C7–C8	1.433	1.398	1.373	1.402	1.401
C8–C3	1.416	1.435	1.457	1.417	1.418
C3–S	1.827	1.763	1.697	1.753	1.750
C4–N	1.369	1.355	1.314	1.392	1.388

pled. Alternatively, from the molecular orbital approach, the bonding pattern in Figure 4 is also consistent with strong delocalization of a pair of electrons from a formal Fe^0 onto the LUMO of the neutral iminothione, *o*-(S)(NH)C_6H_4, ligand. The HOMO of complex **4** (see Figure 5) shows substantial similarity to the LUMO of the neutral thione ligand (see Figure 6). Likewise, the SOMO of the free ligand in the radical anion form is also similar to the HOMO of the complex. If the better description is a -1 π-radical ligand antiferromagnetically coupled to a Fe^{I} radical, one would expect to find a low-lying triplet state and a spin-unrestricted singlet state with lower energy than the spin-restricted one.[19]

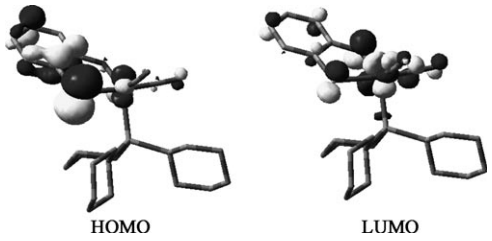

Figure 5. Frontier molecular orbitals (HOMO, left, and LUMO, right, isovalue = 0.05) of complex **4** obtained from DFT calculations.

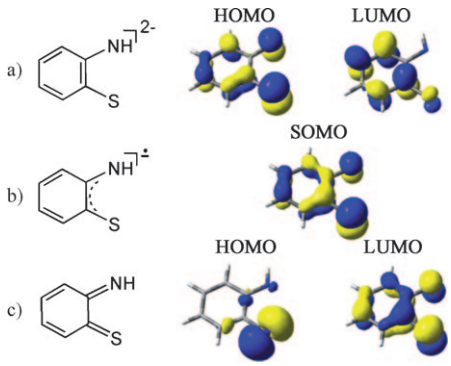

Figure 6. Frontier orbitals (isovalue = 0.05) of the free ligand forms: a) NS^{2-}, 2-amidothiophenolate; b) NS^{-}, 2-iminothionebenzosemiquinonate; and c) NS^{0}: 6-iminocyclohexa-2,4-dienethione.

In fact, calculations find a triplet state that is 14.2 kcal mol^{-1} above the singlet and attempts to find a low-energy, spin-unrestricted singlet state failed because the unrestricted singlet produced essentially the same energy and orbitals as the restricted calculation. Similar results obtained by calculations with the TPSS functional supported the conclusions from those with the B3LYP functional (See Table S1 for details). Thus, all the results point to a delocalized description with a charge distribution like $Fe^{I}(NS^{-1})$ but without significant diradical character.

Mössbauer studies: In order to experimentally probe the oxidation state of iron, Mössbauer spectroscopy was performed. Complexes **4**, **5**, and **6** exhibited sharp quadrupole doublets (see Supporting Information, Figure S3) in a magnetic field of 0.03 T, at 6 K. The values of the isomer shifts (Table 2) are negative and are lower than those observed for low-spin Fe^{II} sites, and in a range expected for low-spin Fe^{I} and Fe^{0} complexes. An Fe^{I} center, particularly for complexes **4** and **5**, would be consistent with the DFT calculations which indicate substantial electron delocalization between the Fe and the NS ligand. Several low-spin ferrous mono- and dicarbonyl complexes (e.g., $[(\eta^5\text{-}C_5Me_5)Fe^{II}(CO)_2(CN)]$ and $[(\eta^5\text{-}C_5H_5)Fe^{II}(CO)(CN)_2]^-$ in Table 2), studied with Mössbauer spectroscopy as reference points for Fe^{II} compounds, show small and positive isomer shifts.[20] The iron carbonyl pyridonate complex reported by Hu, et al., exhibits $\delta = 0.10(2)$ mm s^{-1} and $\Delta E_Q = 0.48(2)$ mm s^{-1} and was assigned as Fe^{II}.[12] Notably, the definitive Fe^{II} complex, *fac*-$[FeI_2(CO)_3PMe_3]$ (**7**),[21] exhibits very similar Mössbauer parameters to those of the [Fe]-H_2ase (see Table 2). The isomer shift of the latter, $+0.06$ mm s^{-1} is consistent with a low-spin Fe^{II} assignment.[5] Thus, although the first coordination sphere donors of complexes **4**, **5** and **6** would suggest close resemblance to the [Fe]-H_2ase active site, their electronic properties as revealed by Mössbauer spectroscopy and DFT calculations described above clearly correspond to a state that is more reduced than Fe^{II}.

Table 2. Selected Mössbauer parameters at 6 K, in an applied magnetic field of 0.03 T.

Complex	δ [mm s^{-1}]	ΔE_Q [mm s^{-1}]
4	−0.078(6)	1.05(1)
5	−0.053(6)	1.03(1)
6	−0.0104(6)	1.00(1)
7[21]	0.065	0.70
$[Cp^*Fe^{II}(CO)_2(CN)]$[20]	0.076	1.97
$[CpFe^{II}(CO)(CN)_2]^-$[20]	0.22	1.85
HMD[5]	0.06	0.65

Chemical properties: In contrast to the [Fe]-H_2ase active site which readily binds extrinsic CO to yield a facial tricarbonyl species, only complex **4** showed any tendency to (weakly and reversibly) take up CO at 1 bar. Neither did complex **4** show reactivity with other Lewis bases such as

PPh_3 and Et_3N. Nevertheless, in the presence of the strong acid, $Et_2O{\cdot}HBF_4$, and CO (1 bar) solutions of complex **4** in acetone (or THF) undergo a color change from dark brown to orange with concomitant ν(CO) spectral changes indicating that stoichiometric CO binding occurs (see Figure 7 and

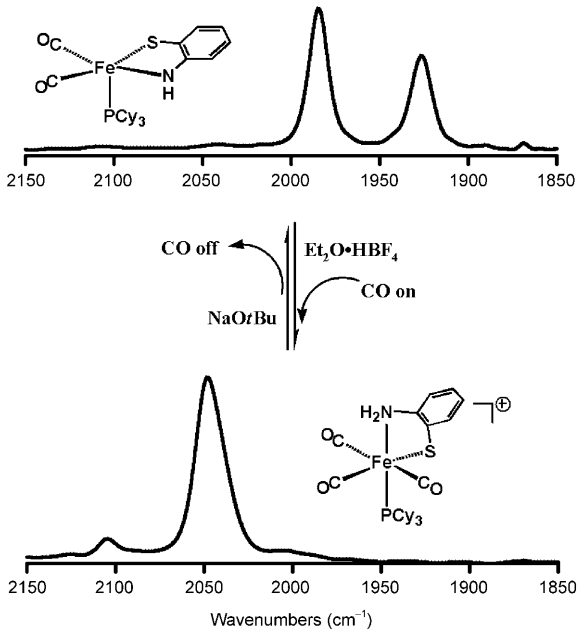

Figure 7. Protonation/deprotonation of complex **4** in the presence of exogeneous CO to yield **4**(CO)-H^+.

Supporting Information, Figure S4). On deprotonation with Et_3N, CO is lost and complex **4** is quantitatively regenerated. While this CO adduct was not isolated, the ν(CO) bands at 2102(w) and 2046(vs) cm^{-1} are, in position and pattern, nearly identical to that of the well-characterized *mer*-$[Fe(CO)_3(I)_2P(OEt)_3]$ complex (2102(w) and 2052(vs) cm^{-1} in CH_2Cl_2 solution, see Supporting Information, Figure S5).[21] Notably, the ν(CO) IR band patterns of the facial isomers within this series are distinctly different from that of the meridional.[22] Hence we propose a tricarbonyl species, *mer*-$[(H\text{-}NS)Fe(CO)_3(PCy_3)]^+$ or **4**(CO)-H^+ with structure as shown in Figure 7 is the product of this reaction.

In a ^{13}CO atmosphere (1 bar), concomitant CO uptake and $^{12}CO/^{13}CO$ exchange occurred within 15 min under the same conditions as above to form [*mer*-(H-NS)Fe-$(^{13}CO)_3PCy_3]^+$ (2056(w) and 2002(vs) cm^{-1} in acetone solution, see Supporting Information, Figure S6). Subsequent treatment with Et_3N reclaimed complex **4** completely ^{13}CO labeled (1982(s), and 1938(s) cm^{-1} in acetone solution) within 10 min. Notably, this is a much more facile labeling process than by the direct $^{12}CO/^{13}CO$ exchange of complex **4** (see Supporting Information, Figure S7). This ^{13}CO exchange with intrinsic CO's of **4**(CO)-H^+ differs from what is observed for the [Fe]-H_2ase active site in the presence of ^{13}CO. The uptake of ^{13}CO by the active site does not result in scrambling, a fact that possibly relates to rigidity of the Fe^{II} site in the protein matrix.[4]

Such a change in electrophilicity of a formally d^6 metal ion on ligand protonation has precedent. Most recently, Heiden and Rauchfuss noted that N-protonation of a diamido ligand chelated to Ir^{III} "redirects π-bonding" resulting in several stable 18-electron base/Ir^{III} adducts, including evidence for η-$^2H_2$ binding and activation.[23] From DFT computations here, the protonation of complex **4** occurs at nitrogen of the NS ligand, and induces a change in the structure of the **4**-H^+ complex relative to that of **4**. Optimized structures of N-protonated isomers of the **4**-H^+ complex (Figure 8) find that as a result of the pyramidality of the amino nitrogen, the NS ligand binding is relaxed such that the $[(H\text{-}NS)Fe(CO)_2(PCy_3)]^+$ or **4**-H^+ complex is a more regular square pyramid. Particularly in the isomers, **4**-H^+ (a) and **4**-H^+ (b) (Figure 8) the C_6H_4SN plane of the ligand is nearly coplanar with the NFeS plane. That is, the structure is now that expected for a coordinatively unsaturated Fe^{II}, d^6 complex and the bonding pattern in the C_6H_4 ring of the N-protonated NS ligand in the calculated **4**-H^+ indicates its aromaticity (see Supporting Information, Figure S2).[18] Frontier molecular orbitals of one isomer are also given in Figure 8. Consistent with protonation-induced electrophilici-

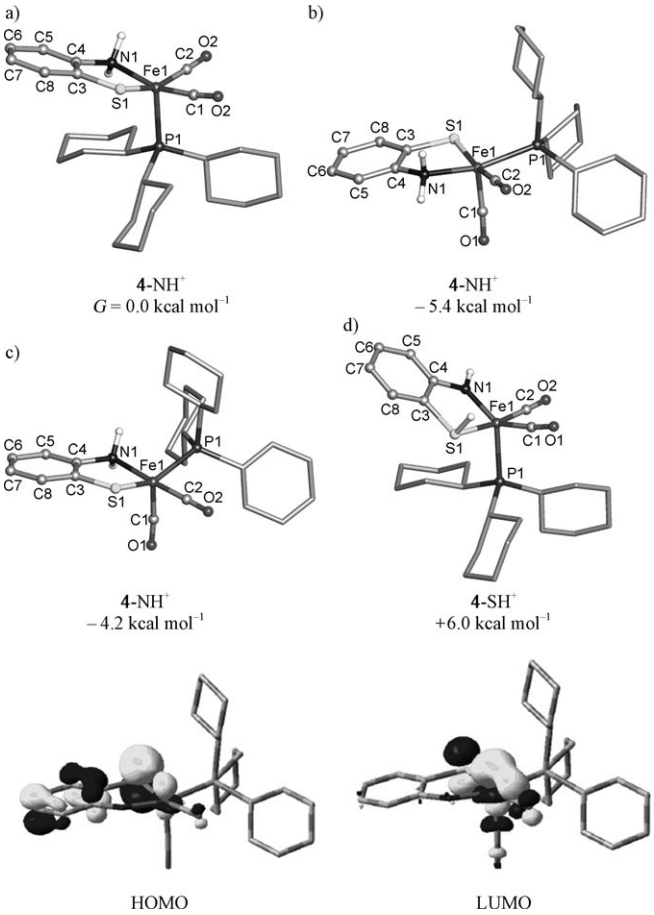

Figure 8. Top: DFT optimized structures and relative energy of the isomers of **4**-NH^+ and a tautomer, **4**-SH^+ (isomer **a** of **4**-NH^+ is defined as $G = 0.0$ kcal mol^{-1}). Bottom: Calculated frontier orbitals (isovalue = 0.05) of **4**-NH^+ (b).

ty at iron, the LUMO of **4**-H$^+$ shows considerable iron character (calculated to contribute 47.6% to the LUMO).

According to the computational result (Figure 8), the lowest energy isomeric form of **4**-H$^+$ is N-protonated (**b** in Figure 8) with the endogenous CO's in the apical/basal positions (similarly to the approximate square pyramidal structure of complex **5**); the open site is *trans* to a CO. Uptake of CO at that site would lead to the meridonal isomer, as opposed to the facial isomer. As we have yet to isolate and characterize complex **4**-H$^+$ in the absence of CO, we rely on computations to relate the neutral complex **4** to **4**(CO)-H$^+$.

Further calculations indicate that the presumed kinetic product *mer*-[(H-NS)Fe(CO)$_3$(PCy$_3$)]$^+$ or **4**(CO)-H$^+$ is also the thermodynamically favored isomer. That the facial isomer is observed in the CO-inhibited state of the [Fe]-H$_2$ase likely reflects both the difference in first coordination sphere donors as well as the restrictions within the protein matrix.[4]

Conclusion

The extreme π-delocalizing or non-innocent ligand as found in the 2-amidothiophenolate ligand described above provides access to a pentacoordinate iron dicarbonyl but renders the iron insufficiently electrophilic to perform as expected for a coordinatively unsaturated d^6, Fe^{II} center.[24,25] DFT computations suggest that as a result of extensive ligand/iron orbital overlap in the frontier molecular orbitals of the pentacoordinate complexes **4** and **5**, the iron is substantially less positive than Fe^{II}, a conclusion that agrees with Mössbauer results. In addition, the differences noted between the pentacoordinate dicarbonyl iron complexes **4** and **5**, and the [Fe]-H$_2$ase enzyme active site, further confirm the oxidation state assignment of Fe^{II} to the latter. The flexibility of the π-character in complex **4** is illustrated by the effect of ligand-based protonation that decreases the electron density at iron, engendering CO uptake and the production of an 18-electron, hexacoordinate complex as expected for d^6, Fe^{II}, and as seen in the [Fe]-H$_2$ase enzyme active site. Whether the synthetic analogue can be further tuned to bind and activate H$_2$ remains to be seen.

Experimental Section

Details of the preparation of complexes **4**, **5**, and **6** are described in the Supporting Information.

As example, that of [(NS)Fe(CO)$_2$PCy$_3$] (**4**) is given here: To a mixture of [FeI$_2$(CO)$_3$PCy$_3$] (reported in ref. [21]) (300 mg, 0.45 mmol) and 2-aminothiophenol (57 mg, 0.45 mmol) in THF (30 mL) was dropwise added 2 equiv of sodium *tert*-butoxide (87 mg, 0.9 mmol in 30 mL THF) over the course of 3 h. The reaction was monitored by IR to completion. THF was removed under vacuum and the residual dark solids were extracted with diethyl ether (30 mL). The organic solution was dried under vacuum and the residue washed with pentane (2×10 mL) to remove byproduct [Fe(CO)$_3$(PCy$_3$)$_2$] (1960(sh) and 1952(s) cm^{-1} in Et$_2$O). The crude product was re-dissolved in Et$_2$O (20 mL) and on cooling at −30 °C, afforded dark crystals of complex **4** suitable for all characterizations (160 mg, 70%). ^{1}H NMR (CD$_2$Cl$_2$): δ = 10.12 (s, 1H, PhN*H*S), 7.82 (s, 1H, *Ph*NHS), 7.47 (s, 1H, *Ph*NHS), 7.09 (s, 2H, *Ph*NHS), 2.08 (br, 3H, Cy), 1.75 (br, 12H, Cy), 1.60 (br, 6H, Cy), 1.06 ppm (br, 12H, Cy); ^{31}P NMR (CD$_2$Cl$_2$): δ = 89.59 ppm (s); IR (CH$_2$Cl$_2$): $\tilde{\nu}$ = 1985(s), 1927(s) cm^{-1}; elemental analysis calcd (%) for C$_{26}$H$_{38}$FeNO$_2$PS: C 60.6, H 7.43, N 2.72; found (C 61.2, H 7.56, N 2.68.

The syntheses of complexes **5** and **6**, were the same as for **4**; isolation and purification, however, differ for each compound. Complete details for **4**, **5**, and **6** (and the byproduct, [Fe(CO)$_3$(PPh$_3$)$_2$] are given in the Supporting Information.

Theoretical details: DFT calculations were performed using a hybrid functional [the three parameter exchange functional of Becke (B3)[26] and the correlation functional of Lee, Yang, and Parr (LYP)[27] (B3LYP) as implemented in Gaussian 03.[28] The effective core potentials and associated basis set of Hay and Wadt (LANL2DZ),[29,30] were used on the iron, sulfur and phosphorus atoms. For iron, the two outermost p functions were replaced by the reoptimized 4p functions as suggest by Couty and Hall.[31] For sulfur and phosphorus, the basis set was augmented by the d polarization function of Höllwarth et al.[32] All carbon, nitrogen, oxygen and hydrogen atoms were represented using Dunning's double zeta valence basis (D95),[33,34] The above functional and basis sets (B3LYP/LANL2DZ&D95) were applied to all species otherwise noted. The geometries of complexes **4** and **5**, **6** as well as other species were fully optimized and confirmed as minima by analytical frequency calculations at the same levels.

In order to thoroughly confirm the structural energetic and degree of diradical character in complexes **4**–**6** and to verify the conclusions from B3LYP/LANL2DZ&D95 calculations, additional calculations were carried out for complex **4** in larger basis sets (Dunning's correlation-consistent polarized valence double-ζ basis set, cc-pVDZ)[35] and with the TPSS functional (see Supporting Information, Table S1).[36]

X-ray diffraction studies: CCDC 743744 and 743745 contain the supplementary crystallographic data for this paper. These data can be obtained free of charge from The Cambridge Crystallographic Data Centre via www.ccdc.cam.ac.uk/data_request/cif.

Acknowledgements

We acknowledge financial support from the National Science Foundation (CHE-0616695 and CHE-0910679 to M.Y.D. and CHE-0541587 and CHE-0910552 to M.B.H.) and The Welch Foundation (A-0924 to M.Y.D. and A-0648 to M.B.H.). The China Scholarship Council provided salary for B.L. C.V.P., who acknowledges support from the National Science Foundation (CHE-0421116) for purchase of the Mössbauer spectrometer and the Summer Fellows program at Ursinus College for Summer research support for her and A.B., is the corresponding author for the Mössbauer spectroscopy. We appreciate helpful discussions with D. J. Darensbourg.

[1] J. C. Fontecilla-Camps, A. Volbeda, C. Cavazza, Y. Nicolet, *Chem. Rev.* **2007**, *107*, 4273–4303.
[2] W. Lubitz, E. J. Reijerse, J. Messinger, *Energy Environ. Sci.* **2008**, *1*, 15–31.
[3] C. Tard, C. J. Pickett, *Chem. Rev.* **2009**, *109*, 2245–2274.
[4] E. J. Lyon, S. Shima, R. Boecher, R. K. Thauer, F. W. Grevels, E. Bill, W. Roseboom, S. P. J. Albracht, *J. Am. Chem. Soc.* **2004**, *126*, 14239–14248.
[5] S. Shima, E. J. Lyon, R. K. Thauer, B. Mienert, E. Bill, *J. Am. Chem. Soc.* **2005**, *127*, 10430–10435.
[6] S. Shima, R. K. Thauer, *Chem. Rec.* **2007**, *7*, 37–46.
[7] S. Shima, O. Pilak, S. Vogt, M. Schick, M. S. Stagni, W. Meyer-Klaucke, E. Warkentin, R. K. Thauer, U. Ermler, *Science* **2008**, *321*, 572–575.
[8] S. Vogt, E. J. Lyon, S. Shima, R. K. Thauer, *J. Biol. Inorg. Chem.* **2007**, *13*, 97–106.

[9] T. Hiromoto, K. Ataka, O. Pilak, S. Vogt, M. S. Stagni, W. Meyer-Klaucke, E. Warkentin, R. K. Thauer, S. Shima, U. Ermler, *FEBS Lett.* **2009**, *583*, 585–590.
[10] X. Yang, M. B. Hall, *J. Am. Chem. Soc.* **2009**, *131*, 10901–10908.
[11] X. F. Wang, Z. M. Li, X. R. Zeng, Q. Y. Luo, D. J. Evans, C. J. Pickett, X. M. Liu, *Chem. Commun.* **2008**, 3555–3557.
[12] B. V. Obrist, D. F. Chen, A. Ahrens, V. Schunemann, R. Scopelliti, X. L. Hu, *Inorg. Chem.* **2009**, *48*, 3514–3516.
[13] A. M. Royer, T. B. Rauchfuss, D. L. Gray, *Organometallics* **2009**, *28*, 3618–3620.
[14] J. M. Smith, R. J. Lachicotte, P. L. Holland, *Organometallics* **2002**, *21*, 4808–4814.
[15] W.-F. Liaw, N.-H. Lee, C.-H. Chen, C.-M. Lee, G.-H. Lee, S.-M. Peng, *J. Am. Chem. Soc.* **2000**, *122*, 488–494.
[16] E. J. Lyon, S. Shima, G. Buurman, S. Chowdhuri, A. Batschauer, K. Steinbach, R. K. Thauer, *Eur. J. Biochem.* **2004**, *271*, 195–204.
[17] A. W. R. Addison, T. Nageswara, J. Reedijk, J. van Rijn, Verschoor, C. Gerrit, *J. Chem. Soc. Dalton Trans.* **1984**, 1349–1356.
[18] D. Herebian, E. Bothe, E. Bill, T. Weyhermuller, K. Wieghardt, *J. Am. Chem. Soc.* **2001**, *123*, 10012–10023.
[19] V. Bachler, G. Olbrich, F. Neese, K. Wieghardt, *Inorg. Chem.* **2002**, *41*, 4179–4193.
[20] C. V. Popescu, Ph.D. Thesis, Carnegie Mellon University (Pittsburgh), **2000**.
[21] B. Li, T. Liu, C. Popescu, A. Bilko, M. Y. Darensbourg, *Inorg. Chem.* **2009**, *48*, 11283–11289.
[22] M. Pankowski, M. Bigorgne, *J. Organomet. Chem.* **1977**, *125*, 231–252.
[23] Z. M. Heiden, B. J. Gorecki, T. B. Rauchfuss, *Organometallics* **2008**, *27*, 1542–1549.
[24] P. G. Jessop, R. H. Morris, *Coord. Chem. Rev.* **1992**, *121*, 155–284.
[25] G. J. Kubas, *Chem. Rev.* **2007**, *107*, 4152–4205.
[26] A. D. Becke, *J. Chem. Phys.* **1993**, *98*, 5648–5652.
[27] C. Lee, W. Yang, R. G. Parr, *Phys. Rev. B* **1988**, *37*, 785.
[28] Gaussian 03, Revision B.04, M. J. Frisch, G. W. Trucks, H. B. Schlegel, G. E. Scuseria, M. A. Robb, J. R. Cheeseman, J. A. Montgomery, Jr., K. N. Kudin, J. C. Burant, J. M. Millam, S. S. Iyengar, J. Tomasi, V. Barone, B. Mennucci, M. Cossi, G. Scalmani, N. Rega, G. A. Petersson, H. Nakatsuji, M. Hada, M. Ehara, K. Toyota, R. Fukuda, J. Hasegawa, M. Ishida, T. Nakajima, Y. Honda, O. Kitao, H. Nakai, M. Klene, X. Li, J. E. Knox, H. P. Hratchian, J. B. Cross, C. Adamo, J. Jaramillo, R. Gomperts, R. E. Stratmann, O. Yazyev, A. J. Austin, R. Cammi, C. Pomelli, J. W. Ochterski, P. Y. Ayala, K. Morokuma, G. A. Voth, P. Salvador, J. J. Dannenberg, G. Zakrzewski, S. Dapprich, A. D. Daniels, M. C. Strain, O. Farkas, D. K. Malick, A. D. Rabuck, K. Raghavachari, J. B. Foresman, J. V. Ortiz, Q. Cui, A. G. Baboul, S. Clifford, J. Cioslowski, B. B. Stefanov, G. Liu, A. Liashenko, P. Piskorz, I. Komaromi, R. L. Martin, D. J. Fox, T. Keith, MvA. Al-Laham, C. Peng, Y. A. Nanayakkara, M. Challacombe, P. M. W. Gill, B. Johnson, W. Chen, M. Wong, W. C. Gonzalez, J. A. Pople, Gaussian, Inc., Wallingford CT, **2004**.
[29] P. J. Hay, W. R. Wadt, *J. Chem. Phys.* **1985**, *82*, 270–283.
[30] W. R. Wadt, P. J. Hay, *J. Chem. Phys.* **1985**, *82*, 284–298.
[31] M. B. H. Marc Couty, *J. Comput. Chem.* **1996**, *17*, 1359–1370.
[32] A. Höllwarth, M. Böhme, S. Dapprich, A. W. Ehlers, A. Gobbi, V. Jonas, K. F. Köhler, R. Stegmann, A. Veldkamp, G. Frenking, *Chem. Phys. Lett.* **1993**, *208*, 237–240.
[33] J. T. H. Dunning, *J. Chem. Phys.* **1970**, *53*, 2823–2833.
[34] J. T. H. Dunning, P. J. Hay in *Methods of Electronic Structure Theory* (Ed.: H. F. Schaefer III), Plenum Press, New York, **1977**, p. 3.
[35] J. T. H. Dunning, *J. Chem. Phys.* **1989**, *90*, 1007–1023.
[36] J. Tao, J. P. Perdew, V. N. Staroverov, G. E. Scuseria, *Phys. Rev. Lett.* **2003**, *91*, 146401.

Received: September 29, 2009
Published online: January 29, 2010

